DISCOVERY OF INTERSTELLAR ANIONS IN CEPHEUS AND AURIGA

M. A. CORDINER[1], S. B. CHARNLEY[1], J. V. BUCKLE[2], C. WALSH[3], AND T. J. MILLAR[3]

[1] Astrochemistry Laboratory and The Goddard Center for Astrobiology, NASA Goddard Space Flight Center, Code 691, 8800 Greenbelt Road,
Greenbelt, MD 20771, USA; martin.cordiner@nasa.gov
[2] Cavendish Astrophysics Group and Kavli Institute for Cosmology, Institute of Astronomy, University of Cambridge, Madingley Road, Cambridge, CB3 0HE, UK
[3] Astrophysics Research Centre, School of Mathematics and Physics, Queen's University Belfast, Belfast, BT7 1NN, UK

ABSTRACT

We report the detection of microwave emission lines from the hydrocarbon anion C_6H^- and its parent neutral C_6H in the star-forming region L1251A (in Cepheus), and the pre-stellar core L1512 (in Auriga). The carbon-chain-bearing species C_4H, HC_3N, HC_5N, HC_7N, and C_3S are also detected in large abundances. The observations of L1251A constitute the first detections of anions and long-chain polyynes and cyanopolyynes (with more than five carbon atoms) in the Cepheus Flare star-forming region, and the first detection of anions in the vicinity of a protostar outside of the Taurus molecular cloud complex, indicating a possible wider importance for anions in the chemistry of star formation. Rotational excitation temperatures have been derived from the HC_3N hyperfine structure lines and are found to be 6.2 K for L1251A and 8.7 K for L1512. The anion-to-neutral ratios are 3.6% and 4.1%, respectively, which are within the range of values previously observed in the interstellar medium, and suggest a relative uniformity in the processes governing anion abundances in different dense interstellar clouds. This research contributes toward the growing body of evidence that carbon chain anions are relatively abundant in interstellar clouds throughout the Galaxy, but especially in the regions of relatively high density and high depletion surrounding pre-stellar cores and young, embedded protostars.

Key words: astrochemistry – ISM: abundances – ISM: clouds – ISM: molecules – stars: formation

1. INTRODUCTION

Hydrocarbon anions have recently been discovered in the quiescent molecular clouds TMC-1 (McCarthy et al. 2006) and Lupus-1A (Sakai et al. 2010), the carbon-rich asymptotic giant branch star IRC+10216 (Cernicharo et al. 2007; Remijan et al. 2007), the protostars L1527 and L1521F, and the pre-stellar core L1544 (Sakai et al. 2008b; Gupta et al. 2009). The possibility that an appreciable fraction of molecular material in interstellar clouds might be in the form of anions was first suggested by Sarre (1980) and Herbst (1981), who pointed out that carbon chain molecules and other radicals have large electron affinities, leading to large radiative attachment rates such as those measured by Woodin et al. (1980). However, the full significance of anions for astrochemistry is still far from understood, so we seek to address the question of just how widespread anions are in the Galaxy. Apart from the single detection in Lupus (Sakai et al. 2010), all interstellar anion detections to date have been confined to the Taurus molecular cloud complex. The origin of the large observed abundances of polyynes (C_nH, $n = 2$–8) and cyanopolyynes ($HC_{2n+1}N$, $n = 1$–5) in this region (e.g., Cernicharo et al. 1986; Bell et al. 1998; Brünken et al. 2007) is debated, and may be attributable to a young gas-phase chemistry (Herbst & Leung 1989), interactions between gas and dust (e.g., Brown & Charnley 1991), or shocking in cloud–cloud collisions (Little et al. 1978). Walsh et al. (2009) theorized that the observed hydrocarbon anions act as catalysts for the synthesis of increased polyyne and cyanopolyyne abundances. New observations of long carbon chains and anions outside of the Taurus complex will provide tests for these astrochemical models and will provide data for the development of new theories regarding the formation of carbon chains throughout the Galaxy.

Models for anion chemistry are able to reproduce, with reasonable accuracy, the observed abundances of C_6H^- and C_8H^- in TMC-1, IRC+10216, and L1527 (Millar et al. 2007; Remijan et al. 2007; Harada & Herbst 2008; Cordiner et al. 2008). The recent detection of CN^- in IRC+10216 by Agúndez et al. (2010) also matches well the abundance predicted by the chemical model of Cordiner & Millar (2009). However, there are still discrepancies between the modeled and observed anion-to-neutral ratios, especially for C_4H^- (Herbst & Osamura 2008), and the lack of anions in photon-dominated regions (Agúndez et al. 2008) is at variance with the model predictions of Millar et al. (2007). Clearly, our understanding of molecular anion chemistry is incomplete. Anions may be of wider importance in astrophysics; their presence within magnetized, collapsing cores may have consequences for star formation dynamics, through their influence on the ambipolar diffusion rate. Molecular anions, including CH_2CN^-, have been considered as plausible carriers for at least some of the unidentified diffuse interstellar bands (Cordiner & Sarre 2007). Anion abundances are theorized to be sensitive to electron attachment and photodetachment rates (see Millar et al. 2007), and may therefore provide a useful tool for the determination of accurate electron densities and cosmic ray/photoionization rates in astrophysical environments.

Presently, many of the key reactions and rates relevant to molecular anion chemistry, such as those of radiative electron attachment, have not been well studied in the laboratory, and so are poorly constrained or grossly approximated in chemical models. Given the current lack of laboratory experiments and detailed (quantum) theoretical calculations, the only way to constrain these parameters and further our understanding of the role of anions in astrophysics is by radio observations and complementary chemical modeling of molecular anions in various astrophysical environments.

This Letter reports new detections of the carbon chain anion C_6H^- in the vicinity of a young, low-mass protostar in the dense molecular cloud L1251A (in the Cepheus complex) and in the pre-stellar core L1512 (in the Taurus–Auriga complex).

2. OBSERVATIONS

Sources were selected from a set of 16 dense clouds for which HC_3N $J = 10–9$ maps had previously been obtained using the Onsala 20 m telescope between 2005 and 2007 (some of which were published by Buckle et al. 2006). The close chemical relationship between polyynes and cyanopolyynes (see, e.g., Federman et al. 1990; Millar & Herbst 1994) suggests that C_4H and C_6H should be abundant in dense molecular clouds, close to where the HC_3N peaks. Therefore, to improve the chances of successfully detecting C_4H, C_6H, and C_6H^- compared with previous surveys (e.g., Gupta et al. 2009), we targeted the strongest HC_3N emission peaks in these maps, which, due to chemical differentiation (e.g., Buckle et al. 2006; Bergin et al. 2007), are not generally coincident with the locations of peak emission from commonly observed molecules such as NH_3, N_2H^+, or CO (for which maps already exist in the literature). Onsala HC_3N $J = 10–9$ maps of L1251A and L1512 are shown in Figure 1. The adopted coordinates for our anion and carbon chain searches were L1251A: R.A. (2000) = 22:30:40.4, decl. (2000) = +75:13:46; L1512: R.A. (2000) = 5:04:07.1, decl. (2000) = 32:43:09. The L1251A position lies $40''$ from the center of the Class 0 protostar L1251A IRS3 and the L1512 position lies $26''$ from the center of a ($\approx 120''$ wide) pre-stellar core (Di Francesco et al. 2008; Kirk et al. 2005). The positions observed by Gupta et al. (2009; who did not detect C_6H^- in either cloud), are not coincident with our observed positions.

Observations were carried out in the months of 2010 April and June using the NRAO 100 m Green Bank Telescope (GBT).[4] The Ka receiver was used with 50 MHz bandwidth and 8192 channels (corresponding to a channel spacing of ≈ 0.065 km s^{-1}), in each of four spectral windows. In the middle of the observed frequency range (28 GHz), the telescope beam FWHM was $26''$ and the beam efficiency factor was 0.88. We performed deep integrations to search for emission lines from C_4H, C_6H, C_6H^-, and HC_7N. Additional observations were obtained of HC_5N, C_3S, and CH_3CCH. For the compact, spatially isolated source L1512, beam switching (with $78''$ throw) was used, and for the more extended source L1215A, frequency switching was used. Pointing was checked every one to two hr and was typically accurate to within $5''$. Total system temperatures were in the range of 40–60 K.

New maps of HC_3N $J = 10–9$ emission in L1251A and C_4H $N = 9–8$ emission in L1512 were obtained using the Onsala 20 m telescope in 2010 May (shown in Figure 1). The basic observation and reduction techniques were presented by Buckle et al. (2006).

3. RESULTS

The C_6H^- and C_6H spectra observed in L1251A and L1512 are shown in Figure 2. To improve the signal-to-noise ratio for L1251A, the C_6H^- $J = 10–9$ and $J = 11–10$ spectra have been averaged in velocity space.

The observed spectral lines were least-squares fitted using single Gaussians, the parameters for which are given in Table 1. The five hyperfine peaks of the HC_3N $J = 3–2$ transition are well resolved in our spectra, from which we derived gas rotational excitation temperatures (T_{ex}) of 6.2 ± 0.3 K for L1251A and 8.7 ± 0.7 K for L1512 (using Equations (1) and (2) of Savage et al. 2002). These temperatures were used in
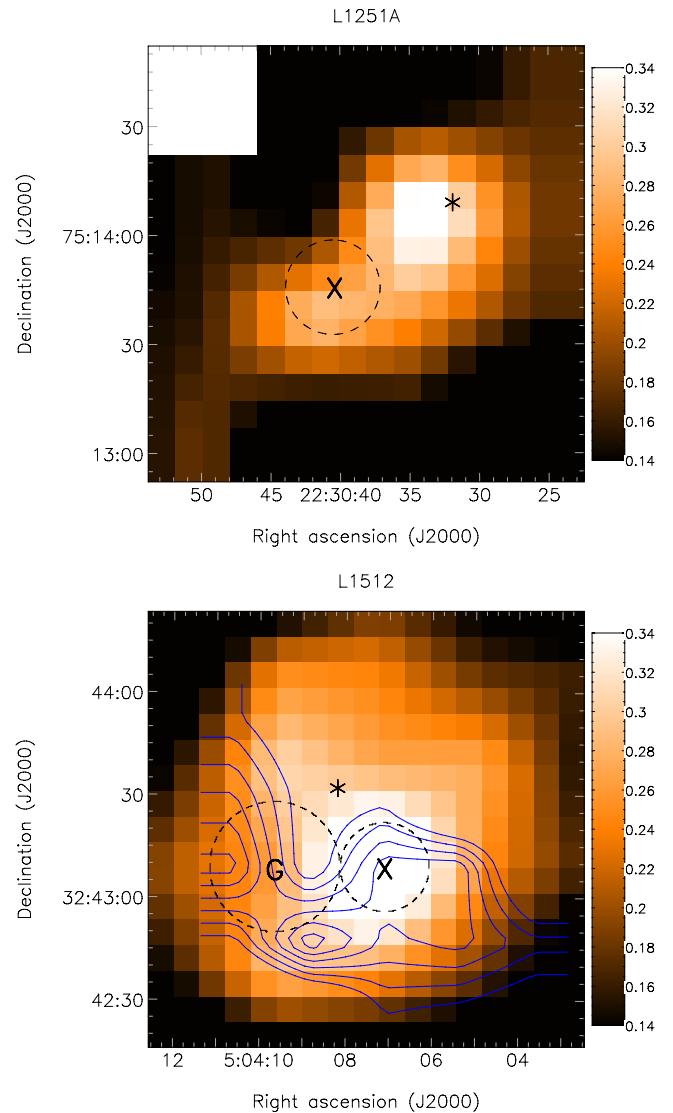
Figure 1. Onsala HC_3N $J = 10–9$ maps of L1251A (top) and L1512 with C_4H $N = 9–8$ contours overlaid (bottom). Scale bar units are K km s^{-1}. C_4H contours show peak antenna temperature, starting at 0.36 K, and increasing in steps of 0.02 K. The observed GBT positions are labeled "X" and location of the Gupta et al. (2009) L1512 anion search is labeled "G". Asterisks show positions of protostar (for L1251A) and submillimeter source (for L1512). Dashed circles represent the GBT beam FWHM of the respective anion searches. Our chosen L1251A position does not coincide precisely with the HC_3N peak because it was based on an earlier, lower-sensitivity map than that shown.

the calculation of the column densities of the observed species assuming LTE and optically thin emission (see for example, Equation (2) of Lis et al. 2002). Where multiple transitions were observed for a given species, the average of the calculated column densities was taken, except for HC_3N, for which only the optically thin $\Delta F = 0$ transitions were used. The HC_3N and other recorded spectra will be presented in a future article. Column densities are given in Table 2.

4. DISCUSSION

Large abundances of carbon-chain-bearing species were observed in both L1251A and L1512. The measured C_4H and C_6H column densities (see Table 2) are similar to those in interstellar clouds with the highest known carbon chain abundances in the Galaxy (see Sakai et al. 2008a, 2009; Gupta et al. 2009). The abundance of carbon chains is also highlighted in L1512

Table 1
Observed Line Parameters

Species Transition[a]	Frequency	L1512				L1251A			
		T_a	v	Δv	$\int T_a dv$	T_a	v	Δv	$\int T_a dv$
C_6H^- $10 - 9$	27537.13	46 (7)	7.09	0.13 (2)	6 (1)	27 (7)	−3.96	0.21 (6)	6 (2)
C_6H^- $11 - 10$	30290.81	18 (7)	7.10	0.16 (7)	3 (1)	24 (7)	−4.00	0.18 (5)	5 (1)
C_4H $3 - 2, 3.5 - 2.5, 3 - 2$	28532.31	715 (50)	7.05	0.15 (1)	114 (8)	383 (45)	−4.05	0.38 (5)	155 (18)
C_4H $3 - 2, 3.5 - 2.5, 4 - 3$	28532.46	931 (50)	7.06	0.15 (1)	149 (8)	486 (34)	−4.04	0.41 (3)	212 (15)
C_6H $10.5 - 9.5, f, 11 - 10$	29109.64	91 (7)	7.26	0.13 (1)	13 (1)	56 (6)	−3.85	0.32 (4)	19 (2)
C_6H $10.5 - 9.5, f, 10 - 9$	29109.69	84 (6)	7.01	0.16 (1)	14 (1)	58 (6)	−4.11	0.27 (3)	17 (2)
C_6H $10.5 - 9.5, e, 11 - 10$	29112.71	99 (7)	7.19	0.14 (1)	15 (1)	58 (6)	−3.94	0.28 (3)	17 (2)
C_6H $10.5 - 9.5, e, 10 - 9$	29112.75	84 (7)	6.96	0.15 (1)	13 (1)	52 (6)	−4.15	0.33 (4)	18 (2)
HC_3N $3 - 2, 3 - 3$	27292.90	671 (65)	7.07	0.12 (1)	86 (11)	246 (24)	−3.99	0.31 (3)	81 (11)
HC_3N $3 - 2, 2 - 1$	27294.07	2102 (52)	6.98	0.16 (0)	358 (9)	967 (22)	−4.10	0.37 (1)	382 (10)
HC_3N $3 - 2, 3 - 2$	27294.29	2769 (53)	7.07	0.16 (0)	472 (9)	1331 (23)	−4.00	0.34 (1)	483 (9)
HC_3N $3 - 2, 4 - 3$	27294.35	3607 (54)	7.15	0.16 (0)	614 (9)	1760 (22)	−3.93	0.39 (1)	732 (10)
HC_3N $3 - 2, 2 - 2$	27296.23	525 (53)	7.08	0.16 (2)	89 (14)	246 (66)	−4.02	0.36 (11)	94 (38)
HC_5N $11 - 10$	29289.15	1364 (40)	7.05	0.21 (1)	305 (8)	998 (22)	−4.05	0.37 (1)	393 (9)
HC_5N $12 - 11$	31951.77	1650 (23)	7.08	0.20 (0)	351 (5)	...	...	...	...
HC_5N $13 - 12$	34614.39	1662 (24)	7.13	0.18 (0)	318 (5)	...	...	...	...
HC_7N $25 - 24$	28199.81	202 (8)	7.20	0.14 (1)	30 (1)	123 (11)	−3.92	0.29 (3)	38 (3)
C_3S $5 - 4$	28903.69	573 (45)	7.16	0.15 (1)	92 (7)	517 (21)	−4.01	0.33 (2)	182 (7)
CH_3CCH $2_1 - 1_1$	34182.76	252 (25)	7.13	0.19 (2)	51 (5)	...	...	...	...
CH_3CCH $2_0 - 1_0$	34183.42	264 (22)	7.15	0.23 (2)	65 (5)	...	...	...	...

Notes. Units of T_a are in mK and velocities are in km s^{-1}, relative to the LSR frame. The 1σ errors on the last quoted digit(s) are given in parentheses.
[a] Transitions are specified as follows: C_6H^-, HC_5N, HC_7N, and C_3S: $J'' - J'$; C_6H: $J'' - J'$, parity, $F'' - F'$; C_4H: $N'' - N'$, $J'' - J'$, $F'' - F'$; HC_3N: $J'' - J'$, $F'' - F'$; CH_3CCH: $J''_K - J'_K$.
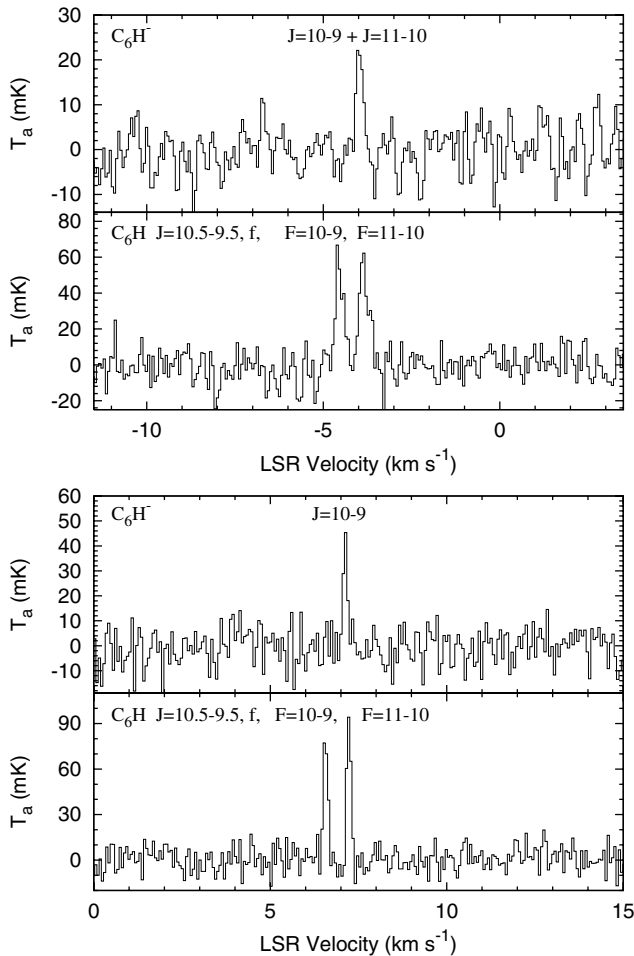

Figure 2. Plot showing (averaged) C_6H^- $J = 10–9$ and $J = 11–10$ spectrum of L1251A (top) and $J = 10–9$ spectrum of L1512 (bottom). The C_6H $J = 10.5–9.5$, f spectra are also shown.

Table 2
Observed Molecular Column Densities

Species	L1512	L1251A
C_6H^-	$2.0 \pm 0.5 \times 10^{10}$	$2.7 \pm 0.7 \times 10^{10}$
C_6H	$4.8 \pm 0.3 \times 10^{11}$	$7.6 \pm 0.8 \times 10^{11}$
C_4H	$9.2 \pm 0.6 \times 10^{13}$	$1.2 \pm 0.1 \times 10^{14}$
HC_3N	$3.0 \pm 0.4 \times 10^{13}$	$2.8 \pm 0.8 \times 10^{13}$
HC_5N	$4.9 \pm 0.1 \times 10^{12}$	$7.5 \pm 0.2 \times 10^{12}$
HC_7N	$1.9 \pm 0.1 \times 10^{12}$	$4.7 \pm 0.4 \times 10^{12}$
C_3S	$1.3 \pm 0.1 \times 10^{12}$	$2.6 \pm 0.1 \times 10^{12}$
CH_3CCH	$3.1 \pm 0.3 \times 10^{13}$	...

Note. Units are cm^{-2}.

by the large CH_3CCH column density, which is comparable to that found in L1527 and TMC-1 (Sakai et al. 2008a). The C_3S column densities in both L1251A and L1512 are somewhat less than previously observed in "carbon-chain-producing regions" by Hirota & Yamamoto (2006). Possible explanations for this include depletion onto dust or reduced elemental sulphur abundances.

The derived C_6H^- column densities of $(2.7 \pm 0.7) \times 10^{10}$ cm^{-2} in L1251A and $(2.0 \pm 0.5) \times 10^{10}$ cm^{-2} in L1512 are similar to those previously observed in other low-mass star-forming cores, e.g., L1521F and L1544 (3.4×10^{10} cm^{-2} and 3.1×10^{10} cm^{-2}, respectively; Gupta et al. 2009), and L1527 (5.8×10^{10} cm^{-2}; Sakai et al. 2007). These values are somewhat less than those observed in the quiescent molecular clouds TMC-1 (1.2×10^{11} cm^{-2}; Brünken et al. 2007) and Lupus-1A (6.5×10^{10} cm^{-2}; Sakai et al. 2010). The anion-to-neutral ratios ($[C_6H^-]/[C_6H]$), however, are approximately in the middle of the previously observed distribution 3.6% $\pm$ 1.3% for L1251A and 4.2% $\pm$ 1.4% for L1512, compared with 1.6% for TMC-1, 2.1% for Lupus-1A, 2.5% for L1544, 4% for L1521F, and 9.3% for L1527. Sakai et al. (2007, 2010) hypothesized that an inverse relationship between H-atom abundance and gas density would result in greater $[C_6H^-]/[C_6H]$ ratios in

denser gas, which may explain the larger ratio found in L1527 where the hydrogen nucleon density n_H is $\sim 10^6$ cm^{-3}, compared to $n_H \sim 10^4$ cm^{-3} in TMC-1. L1251A and L1512 fit this trend—both have $n_H \sim 10^5$ cm^{-3} (Lee et al. 2010; Kirk et al. 2005), and their anion-to-neutral ratios are intermediate between TMC-1 and L1527.

The detection of C$_6$H$^-$ in L1251A is the first reported interstellar anion in a protostar outside of Taurus, and thus shows that the importance of anions must be considered in future studies of the chemistry of star-forming regions throughout the Galaxy.

L1251A and L1512 have similar [C$_6$H]/[C$_4$H] ratios of 0.6% and 0.5%, respectively. These are within the range of values previously measured in interstellar clouds by Gupta et al. (2009).

4.1. L1251A

The L1251A molecular cloud is located in the Cepheus Flare region of low-to-intermediate mass star formation (Kun et al. 2008). Our observed position is 40″ SE of the embedded Class 0 protostar L1251A IRS3, which powers a molecular outflow (Lee et al. 2010). The protostar center is located outside of the 26″ GBT beam (see Figure 1), so emission from its core does not directly influence our observations. However, depending on the radius of its outer boundary (which is likely to be up to a few times 10^4 AU; see, e.g., Jørgensen et al. 2002), gas from inside the protostar envelope is probably responsible for much of the observed molecular emission. It would be of interest to observe the carbon chain (and anion) emission closer to the protostellar core, to determine whether the elevated temperatures there have any impact on the abundances of these species, as has been hypothesized by Sakai et al. (2008a).

Although previous observations have shown relatively large HC$_3$N and HC$_5$N abundances in various parts of the Cepheus complex, our observations constitute the largest reported C$_4$H column density and the first detection of the long-chain species C$_6$H and HC$_7$N in this region. The derived [HC$_7$N]/[HC$_5$N] ratio of 63% is exceptionally high compared with other dense interstellar clouds: the largest value observed in the seven carbon-chain-rich clouds reported by Hirota & Yamamoto (2006) and Sakai et al. (2008a) is 37% in TMC-1. However, there is some uncertainty in the excitation temperatures of these species, as they have been found to differ from each other in TMC-1 by about 1–3 K (e.g., Bell et al. 1998). Assuming that the HC$_5$N rotational temperature is 4–5 K and the HC$_7$N temperature is 5–7 K, and accounting for the optical depth of the HC$_5$N line (0.3), the resulting [HC$_7$N]/[HC$_5$N] ratio in L1251A is 17%–89%. Cernicharo et al. (1986) observed an average ratio of 28% in six cloudlets in Taurus. Thus, the ratio in L1251A is likely to be similar to or larger than in Taurus. These results show that chemical conditions in the Cepheus Flare can be highly conducive to the formation of relatively long carbon-chain-bearing species.

The profiles of the spectral lines in L1251A show a small amount of asymmetry—insufficient to justify fitting multiple Gaussians, but nevertheless indicative of a more complex cloud structure. Although we derive a lower temperature for this cloud than L1512, the lines are broader by approximately a factor of two, which indicates the presence of significant bulk motions of the gases along the line of sight. This may be related to turbulence arising from the L1251A IRS3 outflow, which partially intersects our observed telescope beam.

There is some evidence that the C$_6$H$^-$ lines (with $\Delta v \approx 0.20$ km s^{-1}) are narrower in this source than the lines of the neutral species (with $\Delta v \approx 0.30$ km s^{-1}). A similar phenomenon was also observed by Sakai et al. (2010) in Lupus-1A, who suggested that this may be due to the anion being preferentially located in cooler, denser gas than the neutral. This suggestion seems reasonable on the basis that the rate of radiative electron attachment and, thus, the rate of anion formation is theorized to be proportional to $T^{-1/2}$ and to the electron density (Herbst & Osamura 2008).

4.2. L1512

L1512 is a rather isolated molecular cloud core located in the nearby Taurus–Auriga complex (Ungerechts & Thaddeus 1987). It contains a compact (FWHM $\sim 10^4$ AU) submillimeter source centered around R.A. (2000) = 5:04:08.2, decl. (2000) = +32:43:32 (Di Francesco et al. 2008; Kirk et al. 2005), 26″ NE of our observed position (see Figure 1), which indicates the presence of a dense pre-stellar core covering our telescope beam. Gupta et al. (2009) previously attempted to detect C$_6$H$^-$ at the Benson & Myers (1989) position (30″ east of our observed position, as shown in Figure 1), and they derived an upper limit of 4.8×10^{10} cm^{-2}, which is consistent with our observed column density (see Table 2). They also derived C$_4$H and C$_6$H column densities of $(9 \pm 3) \times 10^{13}$ cm^{-2} and $(5 \pm 2) \times 10^{11}$ cm^{-2}, respectively, which closely match our observed values. Hirota et al. (2009) measured an HC$_3$N column density of 2.5×10^{13} cm^{-2}, 10″ west of our L1512 position, which is in reasonably good agreement with our observed value. The similarities of our observed column densities with those found nearby indicate that polyyne and cyanopolyyne abundances may be less variable than shown by the HC$_3$N map in Figure 1, over spatial scales of $\sim 30''$ (which corresponds to 0.02 pc at the distance of L1512). This implies that the strong, compact peak shown in the HC$_3$N map may arise at least partly as a result of enhanced gas densities and/or temperatures in that region, which (in the case of sub-critical line excitation) would cause increased HC$_3$N $J = 10$–9 emission as a result of increased excitation of the relatively high energy (24 K) $J = 10$ rotational level.

4.3. Comparison and Carbon Chemistry

Located in two distinctly separate parts of the sky (L1251A is ~ 330 pc distant in Cepheus, whereas L1512 is ~ 140 pc distant in Auriga), it is surprising how chemically similar these two clouds are. Apart from HC$_7$N, all of the observed column densities are within a factor of two of each other (see Table 2). This also applies to NH$_3$ (Benson & Myers 1989) and N$_2$H$^+$ (Caselli et al. 2002). The large anion, polyyne, and cyanopolyyne abundances are indicative of an active carbon chemistry, comparable to that observed in other carbon-chain-rich regions of the Galaxy (see, e.g., Hirota & Yamamoto 2006 and Hirota et al. 2009).

Large abundances of unsaturated carbon chains are theorized to occur either in the relatively early stages of dark cloud evolution when carbon is abundant in reactive form (see, for example, Herbst & Leung 1989) or later on during the "freeze-out peak" (Brown & Charnley 1990; Ruffle et al. 1997). In the latter scenario, the lighter, more reactive elements such as atomic oxygen are theorized to freeze out onto the dust grains over time. The loss of oxygen from the gas-phase results in reduced destruction rates for the carbon-chain-bearing species and their associated reagents, giving rise to elevated abundances of these species later on in a dense cloud's evolution.

Over time, two of the primary destructive reactants for organic anions—atomic hydrogen and oxygen—are lost from the gas

phase through conversion on dust grain surfaces to H_2 and H_2O, respectively (Goldsmith & Li 2005; Bergin et al. 2000). This may explain why the C_6H^- anion-to-neutral ratios are greater in denser clouds (including L1521A, L1512, and L1527), than in the quiescent, lower-density clouds TMC-1 and Lupus-1A. Oxygen and hydrogen react quickly with C_6H^- (Eichelberger et al. 2007), so the combined effects of the depletion of O and H in these relatively more dense environments may be responsible for the large observed anion-to-neutral ratios in protostars and pre-stellar cores.

Alternatively, elevated carbon chain abundances could arise as a consequence of selective methane sublimation from dust grain surfaces, as originally investigated by Millar & Freeman (1984) and Brown & Charnley (1991). It is hypothesized that as a protostellar object contracts and begins to heat the surrounding gas, sublimated methane reacts with C^+ to form hydrocarbon ions, which gives rise to a so-called warm carbon chain chemistry (WCCC) via subsequent ion-molecule reactions (see Sakai et al. 2008a; Hassel et al. 2008). Given the close proximity of our observed L1251A position to the protostar IRS3, the WCCC theory may be applicable as a possible explanation for the large hydrocarbon abundances present there.

The location of our L1512 anion detection coincides with the region of CO depletion identified by Buckle et al. (2006). This is also the case for the anion and carbon chain detections in L1521F and L1544 made by Gupta et al. (2009). Thus, the "freeze-out peak" chemistry may be the preferred explanation for the large anion and carbon chain abundances observed in L1512 and similar pre-stellar cores. The presence of hydrocarbon anions is likely to be partly responsible for the large (neutral) polyyne and cyanopolyyne abundances in L1251A and L1512 (see Walsh et al. 2009).

5. CONCLUSION

We have detected the carbon chain anion C_6H^- for the first time in L1251A and L1512. Large column densities of the neutral species C_4H, C_6H, HC_5N, HC_7N, and C_3S were also detected. Combined with the five previous interstellar anion detections by McCarthy et al. (2006), Gupta et al. (2009), and Sakai et al. (2007, 2010), these results show that anions tend to be present in detectable quantities in regions where carbon chains are highly abundant, especially surrounding embedded protostars and pre-stellar cores. The anion-to-neutral ratios $[C_6H^-]/[C_6H]$ are consistently on the order of a few percent and show an apparent positive correlation with density. This implies that a relatively uniform and simple physical/chemical mechanism is responsible for regulating molecular anion abundances in the different interstellar clouds observed so far.

The large polyyne and cyanopolyyne abundances measured in L1251A show that carbon-chain-production processes are rapid in this part of the Cepheus Flare molecular cloud complex, resulting in similar abundances to those found in the Taurus molecular cloud. The observation of abundant C_6H^- in L1251A constitutes the first detection of anions in a protostellar envelope outside of the Taurus–Auriga complex and indicates that anions are likely to be widespread throughout Galactic star-forming regions where carbon chains are present.

The technique of using HC_3N and C_4H as proxies for the detection of less abundant, larger carbon chains and anions shows strong promise as a means for obtaining further detections of these molecules in low-mass star-forming regions in the future.

REFERENCES

Agúndez, M., Fonfría, J. P., Cernicharo, J., Pardo, J. R., & Guélin, M. 2008, A&A, 479, 493
Agúndez, M., et al. 2010, A&A, 517, L2
Bell, M. B., Watson, J. K. G., Feldman, P. A., & Travers, M. J. 1998, ApJ, 508, 286
Benson, P. J., & Myers, P. C. 1989, ApJS, 71, 89
Bergin, E. A., & Tafalla, M. 2007, ARA&A, 45, 339
Bergin, E. A., et al. 2000, ApJ, 539, 129
Brown, P. D., & Charnley, S. B. 1990, MNRAS, 244, 432
Brown, P. D., & Charnley, S. B. 1991, MNRAS, 249, 69
Brünken, S., Gupta, H., Gottlieb, C. A., McCarthy, M. C., & Thaddeus, P. 2007, ApJ, 664, L43
Buckle, J. V., Rodgers, S. D., Wirstrom, E. S., Charnley, S. B., Markwick-Kemper, A. J., Butner, H. M., & Takakuwa, S. 2006, Faraday Discuss., 133, 63
Caselli, P., Benson, P. J., Myers, P. C., & Tafalla, M. 2002, ApJ, 572, 238
Cernicharo, J., Bachiller, R., & Duvert, G. 1986, A&A, 160, 181
Cernicharo, J., Guélin, M., Agúndez, M., Kawaguchi, K., McCarthy, M., & Thaddeus, P. 2007, A&A, 467, 37
Cordiner, M. A., & Millar, T. J. 2009, ApJ, 697, 68
Cordiner, M. A., Millar, T. J., Walsh, C., Herbst, E., Lis, D. C., Bell, T. A., & Roueff, E. 2008, in IAU Symp. 251, Organic Matter in Space, ed. S. Kwok & S. Sandford (Cambridge: Cambridge Univ. Press), 157
Cordiner, M. A., & Sarre, P. J. 2007, A&A, 472, 537
Di Francesco, J., Johnstone, D., Kirk, H., MacKenzie, T., & Ledwosinska, E. 2008, ApJS, 175, 227
Eichelberger, B., Snow, T. P., Barckholtz, C., & Bierbaum, V. M. 2007, ApJ, 667, 1283
Federman, S. R., Huntress, W. T., Jr., & Prasad, S. S. 1990, ApJ, 354, 504
Goldsmith, P. F., & Li, D. 2005, ApJ, 622, 938
Gupta, H., Gottlieb, C. A., McCarthy, M. C., & Thaddeus, P. 2009, ApJ, 691, 1494
Harada, N., & Herbst, E. 2008, ApJ, 685, 272
Hassel, G. E., Herbst, E., & Garrod, R. T. 2008, ApJ, 681, 1385
Herbst, E. 1981, Nature, 289, 656
Herbst, E., & Leung, C. M. 1989, ApJS, 69, 271
Herbst, E., & Osamura, Y. 2008, ApJ, 679, 1670
Hirota, T., Ohishi, M., & Yamamoto, S. 2009, ApJ, 699, 585
Hirota, T., & Yamamoto, S. 2006, ApJ, 646, 258
Jørgensen, J. K., Schöier, F. L., & van Dishoeck, E. F. 2002, A&A, 389, 908
Kirk, J. M., Ward-Thompson, D., & André, P. 2005, MNRAS, 360, 1506
Kun, M., Kiss, Z. T., & Balog, Z. 2008, in Handbook of Star Forming Regions, Vol. I, ed. B. Reipurth (The Northern Sky ASP Monograph Publications, Vol. 4; San Francisco, CA: ASP), 136
Lee, J., et al. 2010, ApJ, 709, 74
Lis, D. C., Roueff, E., Gerin, M., Phillips, T. G., Coudert, L. H., van der Tak, F. F. S., & Schilke, P. 2002, ApJ, 571, L55
Little, L. T., Riley, P. W., MacDonald, G. H., & Matheson, D. N. 1978, MNRAS, 183, 805
McCarthy, M. C., Gottlieb, C. A., Gupta, H. C., & Thaddeus, P. 2006, ApJ, 652, L141
Millar, T. J., & Freeman, A. 1984, MNRAS, 207, 405
Millar, T. J., & Herbst, E. 1994, A&A, 288, 561
Millar, T. J., Walsh, C., Cordiner, M. A., Ní Chuimín, R., & Herbst, E. 2007, ApJ, 662, L87
Remijan, A. J., Hollis, J. M., Lovas, F. J., Cordiner, M. A., Millar, T. J., Markwick-Kemper, A. J., & Jewell, P. R. 2007, ApJ, 664, L47
Ruffle, D. P., Hartquist, T. W., Taylor, S. D., & Williams, D. A. 1997, MNRAS, 291, 235
Sakai, N., Sakai, T., Hirota, T., & Yamamoto, S. 2008a, ApJ, 672, 371
Sakai, N., Sakai, T., Hirota, T., & Yamamoto, S. 2009, ApJ, 702, 1025
Sakai, N., Sakai, T., Osamura, Y., & Yamamoto, S. 2007, ApJ, 667, L71
Sakai, N., Sakai, T., & Yamamoto, S. 2008b, ApJ, 673, L71
Sakai, N., Shiino, T., Hirota, T., Sakai, T., & Yamamoto, S. 2010, ApJ, 718, L49
Sarre, P. J. 1980, J. Chim. Phys., 77, 769
Savage, C., Apponi, A. J., Ziurys, L. M., & Wyckoff, S. 2002, ApJ, 578, 211
Ungerechts, H., & Thaddeus, P. 1987, ApJS, 63, 645
Walsh, C., Harada, N., Herbst, E., & Millar, T. J. 2009, ApJ, 700, 725
Woodin, R., Foster, M. S., & Beauchamp, J. L. 1980, J. Chem. Phys., 72, 4223